

General Disclaimer

One or more of the Following Statements may affect this Document

- This document has been reproduced from the best copy furnished by the organizational source. It is being released in the interest of making available as much information as possible.
- This document may contain data, which exceeds the sheet parameters. It was furnished in this condition by the organizational source and is the best copy available.
- This document may contain tone-on-tone or color graphs, charts and/or pictures, which have been reproduced in black and white.
- This document is paginated as submitted by the original source.
- Portions of this document are not fully legible due to the historical nature of some of the material. However, it is the best reproduction available from the original submission.

NATIONAL AERONAUTICS AND SPACE ADMINISTRATION

Technical Memorandum 33-727

*Radiated Microwave Power Transmission
System Efficiency Measurements*

R. M. Dickinson

W. C. Brown

(NASA-CR-142986) RADIATED MICROWAVE POWER
TRANSMISSION SYSTEM EFFICIENCY MEASUREMENTS
(Jet Propulsion Lab.) 45 p HC \$3.75

N75-26494

CSCL 10A

Unclas

G3/44

24229



JET PROPULSION LABORATORY
CALIFORNIA INSTITUTE OF TECHNOLOGY
PASADENA, CALIFORNIA

May 15, 1975

PREFACE

The basic instrumentation configuration of the total power transmission system of the radiated microwave power transmission system described in this report was originally developed by Raytheon under contract to the NASA Marshall Space Flight Center (MSFC), with William Robinson (now retired) the project engineer. Near the end of that contract (1974), the certified dc-to-dc efficiency measurements were to be made. However, the rectenna was reconfigured by arrangement with William Johnson of MSFC for use by the Jet Propulsion Laboratory (JPL) in preliminary breadboard measurements at the Goldstone Deep Space Communications Complex, with the agreement that the certified system efficiency measurements would be conducted at a later date.

In the interim a new, more efficient, rectenna element configuration and diode was developed under the NASA-JPL contract to Raytheon. The MSFC configuration array has been outfitted with the new JPL rectenna elements. The test measurements and calculation results are due to the efforts of personnel at Raytheon, MSFC, and JPL, supported and encouraged by Sam Fordyce of NASA Headquarters Office of Applications.

The quality assurance certified measurements were performed on March 4, 1975 at the Raytheon Co., New Products Division Building at Waltham, Mass., by JPL and Raytheon Co. engineers.

The technical efforts of JPL were under the cognizance of the Telecommunications Division.

ACKNOWLEDGMENT

Thanks are extended to Bill Robinson and Bill Johnson at Marshall Space Flight Center, Art Paradis of JPL, and Owen Maynard, Henry Chalifour, Bob Girard, Dick Linder, Aline Hinsman, and Bob Sawyer of Raytheon.

CONTENTS

I. Introduction	1
II. Theory	2
III. System Measurement Results and Instrumentation Accuracies	4
IV. System Operation, Performance Monitoring, and Auxiliary Data Points	7
V. Conduct of the Measurements	8
VI. Discussion of System Results	10
VII. Recommendations	11
References	12

APPENDIXES

A. Microwave Power Transmission System Efficiency Test Instrumentation	13
B. Data Sheets	17

FIGURES

1. Block diagram of microwave power transmission system	30
2. Overall laboratory configuration	30
3. Detailed system block diagram	31
4. Magnetron complex	32
5. Magnetron performance characteristics	33
6. Dual-mode horn antenna pattern	33
7. Rectenna complex	33
8. Closeup view of receiving antenna	34
9. Rectenna element radial grouping	35
10. Rectenna wiring format	35

11.	Digi-Cal power meter complex	36
12.	Power meter calibrations	37
13.	System efficiency performance	37
14.	Distribution of system efficiencies (measured and estimated)	38
15.	Average power per element vs radius in the array	38

ABSTRACT

This report presents the measured and calculated results from determining the operating efficiencies of a laboratory version of a system for transporting electric power from one point to another via a wireless free-space radiated microwave beam. The system overall end-to-end efficiency as well as intermediate conversion efficiencies were measured. The maximum achieved end-to-end dc-to-dc system efficiency was 54.18% with a probable error of $\pm 0.94\%$. The dc-to-RF conversion efficiency was measured to be $68.87\% \pm 1.0\%$ and the RF-to-dc conversion efficiency was $78.67 \pm 1.1\%$. Under these conditions a dc power of 45.62 ± 3.57 W was received with a free-space transmitter antenna-receiver antenna separation of 170.2 cm (67 in.).

RADIATED MICROWAVE POWER TRANSMISSION SYSTEM EFFICIENCY MEASUREMENTS

R. M. Dickinson¹ and W. C. Brown²

I. INTRODUCTION

This report presents the measured and calculated results from determining the operating efficiencies of a laboratory version of a system for transporting electric power from one point to another via a wireless free-space radiated microwave beam (Refs. 1 and 2). The system overall end-to-end efficiency as well as intermediate conversion efficiencies were measured.

The overall efficiency measurement includes the effects of inefficiencies associated with converting the input dc power to RF power, forming and radiating the beam of microwaves across the transmission distance, collecting the microwave beam at the power receiving location, and finally reconverting the RF power back to dc power. The end-to-end efficiency is determined from the ratio of output dc power to input dc power of the system.

The certified efficiency determination was undertaken to provide a positive-definite bench mark in the rapidly changing progress in the free-space transmission of power. A preliminary measurement of 48% overall power transmission efficiency was made and reported in Ref. 3.

Knowing accurately the magnitude and exact whereabouts of the various inefficiencies in the system will allow the focusing of development efforts on the largest loss contributors. It will also provide a means for determining rate of progress in developing components of the system.

Instrumentation and measuring techniques and procedures will be developed to aid in future higher power level, longer range system measurements and to facilitate determining system performance and safety monitoring locations and parameter ranges.

¹Jet Propulsion Laboratory

²Raytheon Co.

II. THEORY

The act of transporting dc power via free-space radiated microwaves as illustrated in the simplified block diagram of Fig. 1 involves the following:

- (1) Conversion of the input dc power from the generator into microwaves.
- (2) Forming and radiating the microwave beam in the direction of the receiver.
- (3) Collecting the radiated beam at the receiving site.
- (4) Converting the received RF energy back into dc for delivery to a load.

Figure 2 is a photograph of the laboratory configuration for this test series.

Figure 3 is a detailed block diagram of the actual test configuration showing the elements necessary for power transmission along with the supporting instrumentation to provide detailed measurements and status of the system.

The individual equipments that make up the laboratory system under consideration and their operating conditions and design factors that affect the overall efficiency are as follows:

- (1) The RF generator shown in Fig. 4 or the device that converts the dc source power into RF is an air-cooled, directly heated cathode, permanent magnet magnetron. The heater and blower power will not be charged against the system input power, since by an alternate more efficient design they could be minimized or eliminated, and in a large power system it would be infinitesimal compared to the transported power.

Hence, the system input power will be the product of anode voltage and anode current. Figure 5 is a typical plot of power output, efficiency and frequency versus anode current for the magnetron. The dc-to-RF conversion efficiency is approximately 72% \pm 2%.

- (2) Associated with the magnetron output RF circuitry are an impedance matching device and a terminated circulator to provide for load output protection and optimizing the RF generator load impedance match. These devices account for approximately 4% loss in the magnetron output or -0.177 dB.
- (3) The radiating antenna is a 57-cm diam dual-mode horn (Ref. 4). The estimated I^2R losses, cross-polarization and spillover losses in this element are approximately 1% or -0.04 dB. Figure 6 is a measured pattern of the antenna.
- (4) The propagation medium consists of air at standard temperature and pressure. The loss at the operating frequency of 2450 MHz and for the maximum power density of approximately 1100 mW/cm², which occurs 0.5 m in front of the horn, is negligible.
- (5) The receiving antenna shown in Figs. 7 and 8 is an array of 199 halfwave dipoles arranged in a triangular lattice mounted above a reflecting plane. The estimated collection efficiency of the array is 95%.
- (6) The RF-to-dc converters behind each receiving halfwave dipole consist of a series RF low-pass filter whose output goes to a gallium arsenide Schottky barrier halfwave diode rectifier. Following the diode, an RF bypass filter capacitor acts as part of a tuned circuit impedance transformer to match the low diode impedance to the low-pass filter output impedance. The measured efficiency of these converters is a function of power level and varies up to 87%. The estimated overall aggregate conversion efficiency of the entire array is 85%.

Combining all of the above efficiencies and losses yields an estimated dc-to-dc overall system efficiency of 55%.

Apart from the RF generator and its protective and load matching circuitry, the major factors affecting the transmission efficiency are the alignment of the transmitting and receiving antennas for optimum polarization compatibility and minimizing multipath loss. Also, the receiving

antenna must be optimally impedance matched to operate most efficiently over the range of power densities caused by the transmitting antenna beam spread. The receiving array element impedance match is a function of the dipole impedance termination, separation from adjacent elements, standoff distance from the ground plane, and angle of incidence of the incoming wavefront.

The transmitting antenna must shape the transmitted beam most efficiently to minimize the sidelobe level and yet place most of the power in the main beam without spreading the main beam unduly (such as to require an overly large receiving antenna).

For a given transmission distance and combination of transmitting and receiving antenna areas, an optimum illumination function exists (Ref. 5). For this laboratory setup, the optimum function is approximately Gaussian.

Additionally, the ultimate in efficiency at the receiving or rectenna end of the system could be obtained by having isolated individual loads across each of the 199 half-wave dipole antenna elements that are tailored to present the optimum impedance to each element, taking into account its operating power level position in the array. Having a single output dc load as an operational convenience in this laboratory setup costs more than 4% in system overall efficiency and thus was not utilized. However, to avoid 199 measurements of voltage and current, the array load was consolidated into 22 separate loads. Figures 8 and 9 show how the various rectenna elements are grouped into parallel sets.

III. SYSTEM MEASUREMENT RESULTS AND INSTRUMENTATION ACCURACIES³

The magnetron anode voltage was measured using a 10,000:1 voltage divider whose ratio was set to within $\pm 0.03\%$. The magnetron anode current was measured using a shunt resistor of 1.005Ω calibrated to an accuracy of 0.1% . Both of these quantities were measured using a Hewlett-Packard (HP) Model 3460B digital voltmeter (DVM) with an accuracy of $\pm 0.01\%$.

³ See Appendix A.

Therefore, the input dc power could be measured to an rms accuracy of 0.105%. Unfortunately, the input power uncertainty was approximately six times larger than this figure because of the lack of adequate automatic current regulation in the magnetron power supply. The input power regulation to the magnetron was assisted by manually adjusting a vernier on the high-voltage power supply such as to maintain the current to within ± 1 mA on the current indicator.

The resulting supply voltage was spot checked during the measurement run and at the beginning and end. The highest efficiency record run was made with a $\pm 0.85\%$ peak-to-peak uncertainty (or $\pm 0.6\%$ rms) in input dc power due to combined instrumentation and system drifts.

The output dc power was determined by the summation of the results of the individual voltages and current products across the 22 separate load resistors. The voltages were measured with a HP Model 3440 DVM with an accuracy of $\pm 0.06\%$. The currents were measured with a Fluke Model 8000A digital multimeter with an accuracy of $\pm 0.4\%$.

A detailed analysis to determine the uncertainty in the output power would weigh the instrumentation accuracy in each load measurement by the relative contribution of that load to the total power output. However, because of the varying input power, the output power must be ascribed an uncertainty larger than just the weighted average instrumentation error. Thus, the output power accuracy was taken to be the rss of the input power variation, $\pm 0.6\%$ and the output instrumentation accuracies for a total rss uncertainty of $\pm 0.72\%$.

The RF power was measured by breaking the system chain at the flange on the input side of the waveguide matching section to the dual-mode horn and connecting the waveguide matching section, transition, and water load shown in Figs. 3 and 10.

The Raytheon Digi-Cal power meter was used as an intermediate transfer device to relate the Weston wattmeter reading to the HP-Fluke power meter DVM readout. Since the measurement is a substitution type,

only the constancy of flow rate in the water system is important and not the absolute value.

Figure 11 shows the pre-, post- and day-of-record wattmeter calibrations. The approximately constant offsets between the HP-Fluke and Digi-Cal readings are due to the coupling error of the approximately 50-dB crossguide directional coupler. It is not known for certain what caused the day-to-day variations. As the series of measurements progressed, the magnetron output coupling was changed between each of the daily wattmeter calibrations in order to place its stable operating point at higher current and power levels. The retuning probably affected the harmonic power output which may register differently on the wideband 50-dB coupler HP-Fluke power monitor or may not all be absorbed in the water load Digi-Cal power indicator.

The HP-Fluke power meter calibration data of March 5, 1975 reflect the tuning condition of the magnetron as it was on March 4, 1975, when the highest dc-to-dc efficiency measurements were made. Thus, the determination of the uncertainty in RF power will be based upon the March 5, 1975 dated curve. The peak-to-peak power readings are $\pm 0.8\%$ or $\pm 0.6\%$ rms.

Therefore, the RF power measurement uncertainty will be taken as the rss of $\pm 0.6\%$ due to input power variations as recorded from the HP-Fluke readings along with $\pm 0.5\%$ basic accuracy of the Weston and $\pm 0.1\%$ due to the count ambiguity of the Fluke DVM readout. The net result is an rss uncertainty in the RF power readings of $\pm 0.79\%$.

Summarizing, the input dc power for the highest efficiency record measurement was 914.76 W $\pm 0.61\%$. The corresponding output dc power was 495.62 W $\pm 0.72\%$. Therefore, the system end-to-end dc-to-dc efficiency is

$$\eta_{\text{dc-dc}} = \frac{495.62 \text{ W } \pm 0.72\%}{914.76 \text{ W } \pm 0.61\%} = 54.18\% \pm 0.94\% \text{ p. e.}$$

The RF power measured for the same conditions was 630 W $\pm 0.79\%$, and thus the input dc to RF conversion efficiency

$$\eta_{\text{dc-RF}} = \frac{630 \text{ W} \pm 0.79\%}{914.76 \pm 0.61\%} = 68.87\% \pm 1.0\% \text{ p. e.}$$

The output RF-to-dc reconversion efficiency

$$\eta_{\text{RF-dc}} = \frac{495.62 \text{ W} \pm 0.72\%}{630 \text{ W} \pm 0.79\%} = 78.67\% \pm 1.1\% \text{ p. e.}$$

IV. SYSTEM OPERATION, PERFORMANCE MONITORING, AND AUXILIARY DATA POINTS

In addition to the aforementioned monitoring concerning maintaining the magnetron input power approximately constant, precautions were taken to assure that the RF load impedance presented to the power source (output of circulator) by the dual-mode horn or the water load are approximately the same. Thus, permanent matching sections were affixed to both loads.

The 0.5-dB VSWR of the antenna and the 0.25-dB VSWR of the water load could lead to, at most, a 0.008-dB variation in power transfer for the two conditions.

It had previously been found to be necessary to shield the HP power meter and sensor used in conjunction with the 50-dB coupler in order to prevent error in the reading due to RF entering the ac power leads or coupling through the power sensor cable. Therefore, a battery-powered meter was used that was mounted in an RF gasketed shielded aluminum box affixed to the waveguide flange mounting. (Since absolute accuracy was not required for the power meter used in the VSWR and frequency meter indication functions, it was not shielded.) The battery-powered Fluke DVM connected to the power meter recorder output was used to allow accurate readings to be taken through the screened view port of the RF tight box.

A Microdek microwave leakage meter was used to check for leakage of RF around flanges and to monitor the 10 mW/cm^2 contour around the beam transmission space between horn and rectenna array.

A motor-driven tenth wavelength dipole on a probing arm perpendicular to the vertically polarized beam was used to measure the VSWR of the array. The maximum 1.2-dB VSWR would correspond to -0.022 dB or 1/2% loss in power transmission.

An oscilloscope was used to monitor the ripple in the dc output to insure that excessive ripple would not degrade the digital voltmeter and ammeter readings. The output ripple waveform monitor was also useful to give an indication of magnetron instability due to load conditions. Evidently the extremely tight coupling of the magnetron output required for maximum dc-to-RF conversion efficiently, coupled with the finite isolation provided by the terminated circulator, were inadequate to assure stable single-frequency output for a large range of currents. It required a combination of tuning the magnetron output matching, filament current, and voltage and anode supply careful setting to achieve a somewhat stable 240-mA operating condition.

Additionally, a flap of RF absorbing material was put in place over the mouth of the dual-mode horn at each magnetron turn-on in order to preclude any severe transients of high-intensity RF from damaging the rectenna diodes. Once the magnetron was operating stably the absorbing flap was removed. However, further system operating experience has found this precaution to be unnecessary.

During the conduct of the measurements several diode and circuit mechanical problems were found and corrected or replaced between data logging runs. Once corrected, however, the data runs could be very satisfactorily repeated.

V. CONDUCT OF THE MEASUREMENTS

Several days were spent in trimming and adjusting the nominal operating points of magnetron current and tuning for maximum conversion efficiency, optimizing the impedance match of the horn and water load, optimizing the separation of horn and rectenna array, setting the optimum tuning and ground plane spacing of the rectenna array elements and developing data sheets and measurement sequences. Also, several "bugs" had to be worked out of the magnetron power supply, Digi-Cal and water load as well as the

rectenna array. Additional digit capability in some of the digital voltmeters had to also be obtained.

On March 4, 1975, however, for-the-record data runs were begun in earnest and are shown in Appendix B.

The first data sheet records the comparison of the Digi-Cal readout to the power input monitored by the Weston power meter as applied to the water load system. This data is plotted in Fig. 11.

The second data sheet recorded the magnetron performance and the tracking between the HP-Fluke digital power indicator and the Digi-Cal. This data is plotted in Figs. 5 and 11.

Data sheet page 3 is for the case of 210-mA current into the magnetron, which was thought to represent the optimum dc-to-dc efficiency condition. Runs at 200 and 220 mA were taken to bracket this case. However, after calculation of the end-to-end efficiency as shown in Fig. 12, it was discovered that the 220-mA case resulted in higher efficiency. Thus, a 230-mA case was run. Again higher efficiency was obtained, and it was decided to run at 240 mA. This required retuning the magnetron. After the first 240-mA run recorded on data sheet 7 it was recognized that a diode in set No. 7 of the array was performing improperly. After replacement the data set on sheet 8 was recorded. The data on this page resulted in the highest dc-to-dc efficiency recorded.

After the data run of sheet 8, the spacing between the horn and rectenna array was increased in order to promote a more uniform power density across the rectenna array (however, at the expense of allowing more power to leak past the edges). It was hoped that the higher conversion efficiency and larger magnitude of power associated with the higher power level applied to the edge elements would more than offset the increased spillover losses.

Nevertheless, only 240 mA of current could be stably applied to the magnetron with the power supply available and the resulting power transfer efficiency was lower than previously.

Since the earlier wattmeter calibrations had been done for lesser magnetron current tuning conditions it was felt that higher power level recalibrations should be made. Data sheets 9A and 9B were taken the following day after the horn was disconnected and the water load, Digi-Cal power-meter, and Weston power meter combination was reconnected.

VI. DISCUSSION OF SYSTEM RESULTS

Figure 13 shows the best estimate of the distribution of the system losses. The greatest area for efficiency improvement is in the dc-to-RF converter. (The current magnetron is one designed for the rugged requirements of consumer microwave oven use, and thus the efficiency performance is not a paramount design parameter.) Tubes developed specifically for this service could greatly increase the system performance.

The area with the next largest area for improvement is the RF-to-dc converter. The current diodes have a maximum RF-to-dc conversion efficiency of $87\% \pm 1.5\%$. New materials and designs could improve the efficiency and power handling characteristics.

The circulator could be removed from the system in order to decrease losses. However, there would be an increased risk to the dc-to-RF converter since there would be no isolation of the converter from the load. A newer generation designed system may be able to structure the power supply and dc-to-RF converter to enable them to absorb or tolerate the mismatch reflections from the rectenna array that result at lower or higher than designed RF power levels and also in case the rectenna dc load is mismatched.

The rectenna array edge treatment and other characteristics, such as load distribution management, could possibly be improved to allow higher collection efficiency. Figure 14 is a plot of the theoretical and measured average power per element as a function of radius in the rectenna array.

VII. RECOMMENDATIONS

If the tests are to be repeated, or in the future as component development efficiency increases are to be inserted in the system for checkout, it is recommended that the power supply be improved to allow for higher regulated current capability. A spectrum analyzer should be connected to a monitor point to allow quantifying the harmonic content of the dc-to-RF converter output.

A more efficient dc-to-RF converter should be used, as the magnetron was the largest single-loss item in the system.

A new load distribution management scheme should be configured to allow testing the system operating characteristics with a varying single load. In addition, a single load would allow the possibility of developing a bridge instrumentation arrangement to ratio the output and input dc power so as to read efficiency directly. Optimum component tweaking to effect maximum efficiency would be more readily obtained.

The surrounding unused reflector area near the edge of the rectenna array needs to be investigated to determine the best configuration (reflecting, absorbing, or transmitting) for maximum efficiency.

Some of the waveguide components and transitions may be omitted to decrease losses. For example, the dual directional coupler could serve the function of the slotted guide if it were fitted with ratiometer capability. A low-pass filter should be used to minimize harmonic effects. RF conducted power meters that could work unambiguously when immersed in an ambient RF field would make measurements less difficult. A waveguide switch to facilitate changing from horn to water load could cut down on time drift uncertainties. A large-diameter rectenna would tend to increase the absorption efficiency, because it would reduce the radial power density gradient and allow the rectenna elements near the array edge to operate at higher individual collection efficiency.

REFERENCES

1. Brown, W. C., "The Technology and Application of Free-Space Power Transmission by Microwave Beam," in IEEE Proceedings, Vol. 62, No. 1, pp. 11-25, January 1974.
2. Brown, W. C., "Free Space Microwave Power Transmission Study, Phase II," Raytheon Report PT-3539 under Contract NAS-8-25374.
3. Brown, W. C., and Kim, C. K., "Recent Progress in Power Reception Efficiency in a Free Space Microwave Power Transmission System," presented at the IEEE-MTT International Microwave Symposium, Atlanta, Ga., May 1974.
4. Potter, P. D., "A New Horn Antenna with Suppressed Sidelobes and Equal Beamwidths," Microwave Journal, pp. 71-78, June 1963.
5. Goubau, G., and Schwering, F., "Free-Space Beam Transmission," in Microwave Power Engineering, Vol. 1, pp. 241-255, Editor, E. C. Okress, Academic Press, New York, 1968.

APPENDIX A

**MICROWAVE POWER TRANSMISSION SYSTEM
EFFICIENCY TEST INSTRUMENTATION**



DQA 75-199
DATE March 7, 1975

TO K. Anhalt *AK* SEC. 151
FROM A. Faradis EXT. 5437 SEC. 151
SUBJECT Raytheon - CT 953968 - Microwave Power Transmission System
Efficiency Test Instrumentation

Instrumentation used to perform JPL certification test of DC to DC efficiency on rectenna breadboard sub-array at the Microwave & Power Tube Division, Raytheon Company, Waltham, MA, on 3-4-75 and 3-5-75. Item numbers refer to system block diagram instrument placement.

ITEM

1. Raytheon DC Power Supply
2. Voltage Divider 10,000 to 1
3. Digital Voltmeter H/P 3460B
4. 1.005 ohms Shunt Dale RH-50
5. Magnetron Hitachi 2M71
6. Power Meter H/P 435A
7. Digital Voltmeter Fluke 8000A
8. Power Meter Narda 447
9. Frequency Meter PRD Electronics Inc. Type LS-518
10. Calorimetric System Raytheon Digi-Cal C1000A
11. Wattmeter Weston 310
12. Digital Voltmeter Fluke 8000A
13. Digital Voltmeter H/P 3440A

PRECEDING PAGE BLANK NOT FILMED

JPL 0893-S R 5/71

All instrumentation and test set-ups were inspected by JPL QA. Instruments affecting accuracy of data recorded to determine DC to DC efficiency were found to be within calibration. Calibration accuracy is directly traceable to the National Bureau of Standards within Raytheon except for the Weston 310 Wattmeter, which is traceable to the NBS through certificate of calibration from the manufacturer.

Non-calibrated "indication only" instrumentation was inspected and found to be operationally acceptable.

Performance of the test and recording of the resulting data was witnessed and verified for accuracy by JPL QA.

AP:llc

Distribution

R.B. Crow
R. Dickinson
M. Jacobs
R. Stokely
K. Tate
C.P. Wiggins
QA/DC

APPENDIX B
DATA SHEETS

(PREPARED BY) R. Dickinson	(DATE) 3-8-75	(REPORT NO.)
(CHECKED BY) A. PARADIS	(DATE) 3-4-75	(PROJECT) RXCV DC-RF-DC CERTIFICATION
TITLE 60Hz POWER CALIBRATION		

TIME	WESTON W	DIGI-CAL W	NOTES
0849	500	506	WESTON ON HIGH ^{RANGE} SCALE (F.S. = 1 KW)
	500		WESTON ON LOW RANGE (F.S. = 500 W)
0902	497	502	DIGITAL FWH RATE INDICATED 0.739 PM
0912	500	504	WESTON ON HIGH RANGE AGAIN (F.S. = 1 KW)
0918	520	526	
0919	540	546	
0920	560	566	
0921	580	586	
0923	600	606	

jpl →

(PREPARED BY) R. DICKINSON	(DATE) 3-9-75	(REPORT NO.)
(CHECKED BY) A. PARADIS	(DATE) 3-4-75	(PROJECT) RCLV DC-RF-DC CERTIFICATION
TITLE SYSTEM TRANSFER EFFICIENCY DATA		

SET NO.	TIME	V _{REF} , V	I _{REF} , A	POWERED RE-FLUT	WATTMETER E _h , W	I _h , A	NOTES
JPL 57 0	1036	35.70	.268	569	3.890	210.0 ^{E.T}	FREQ. MHz f ₀ = 2446.0
1		35.14	1.412				VSWR ANTENNA, dB 0.3
2		32.19	1.347				VSWR ARRAY RECTOR, dB 1.0 dB
3		30.75	1.286				HORN-RECTOR SPACING 170.2 CM.
4		59.11	1.165				RIPPLE V _{REF} /V _{DC} 0.7/35
5		25.70	1.080				
6		22.89	.970				
7		42.87	.934				
8		19.53	.827				
9		34.25	.750				
10		31.44	.687				
11		17.65	.584				
12		12.45	.544				
13		24.70	.532				
14		21.35	.471				
15		9.50	.410				
16		17.90	.396				
17		16.70	.373				
18		14.70	.320				
19		6.13	.266				
20		11.20	.362	357	3.000		
JPL 57 21	1041	7.77	.178	367/665	3.838/ 3.336	210.0 ^{E.T}	2446.2

CLASSIFICATION

JPL 0000-3 (REV 11-60)

(PREPARED BY) R. D. KINSON (DATE) 7-9-75 (REPORT NO.)

(CHECKED BY) A. PARADIS (DATE) 3-4-75 (PROJECT) RXCV NC-RF-DC CONVERSION

TABLE SYSTEM TRANSFER EFFICIENCY DATA

SET NO.	TIME	RECEIVED		PULSED OR PULSE	WAVEFORM		NOTES
		V _{SET} , V	I _{SET} , A		FR. FREQ.	I _{MA}	
JPL 07 0	1047	36.03	.275	597	7.870	^{10.6} 280.0	FREQ. MHz f ₀ = 2499.0
1		35.20	1.455				VSWR ANTENNA, dB 0.2
2		37.30	1.395				VSWR ARRAY RECTOR, dB 1.2
3		31.64	1.322				Mod. RECTOR CAPS 170.2 CM.
4		55.76	1.208				RIPPLE V _{IN-TH} /V _{DC} 0.7% _{SSV}
5		26.62	1.116				
6		23.71	1.005				
7		44.11	.956				
8		20.08	.852				
9		35.22	.767				
10		32.37	.700				
11		19.01	.597				
12		12.70	.558				
13		29.65	.545				
14		21.62	.476				
15		9.61	.415				
16		18.12	.400				
17		16.82	.372				
18		14.60	.320				
19		6.11	.263				
20		10.81	.350	597	3.827		
JPL 07 21	1056	7.58	.186	597	3.828	^{10.6} 220.0	

jpl →

PAGE 5 OF 9

(PREPARED BY) R. OIKENSON	(DATE) 3-4-75	(REPORT NO.)
(CHECKED BY) A. PARADIS	(DATE) 3-4-75	(PROJECT) RRLV DC-RF-DC CERTIFICATION
TITLE SYSTEM TRANSFER EFFICIENCY DATA		

SET No.	TIME	V _{SET} , V	I _{SET} , A	INDICATED PA-FLUX	PA AGN FROM Fd, W	T _{LOAD} , °C	NOTES
0	1057	34.09	.259	577	3.826	200.0 ^{±.5}	FREQ. MHz F ₀ = 2449.0
1		33.70	1.766				VSWR ANTENNA, dB 0.3
2		31.92	1.705				VSWR ARRAY RECTOR, dB 0.9
3		29.82	1.290				MAX. RESONANCE SWR 170.2 CM.
4		52.21	1.130				RIPPLE V _{DC} -I _{DC} /V _{DC} 0.4
5		25.07	1.042				
6		22.20	.933				
7		41.92	.892				
8		18.96	.798				
9		33.32	.723				
10		30.67	.665				
11		13.24	.562				
12		12.15	.525				
13		23.80	.519				
14		20.75	.460				
15		9.39	.401				
16		17.62	.386				
17		16.65	.365				
18		14.60	.315				
19		6.07	.260				
20		11.27	.262				
21	1106	7.71	.182	539/536	3.829 3.830	200.0 ^{±.5}	2443.7

CLASSIFICATION

JPL 0000-6 (REV 11-68)

JPL →

(PREPARED BY) R. DICKINSON	(DATE) 3-2-75	(REPORT NO.)
(CHECKED BY) A. PARADIS	(DATE) 3-4-75	(PROJECT) RXCV DC-RF-DC CERTIFICATION
TITLE SYSTEM TRANSFER EFFICIENCY DATA		

SET No.	TIME	RECTIFIED V _{SET} , V	I _{SET} , A	PIVOTATED RE-FLUX	WAVEFORM F _h , Kc	T _h , mA	NOTES
19 7dr 0	1203	36.76	.282	624	3.793	2200	FREQ. 14N9 f ₀ = 2947.8
1		36.04	1.979				VSWR ANTENNA, dB 0.2
2		34.15	1.420				VSWR ARRAY RECTOR, dB 1.10
3		32.52	1.398				NOISE-REJECTION CAPABLE 170.2 CM.
4		57.91	1.272				RIPPLE V _{RE-FL} /V _{DC} 1.2
5		27.19	1.136				
6		29.22	1.020				
7		45.14	.979				
8		20.60	.863				
9		36.20	.788				
10		33.25	.720				
11		19.26	.610				
12		12.92	.566				
13		25.27	.554				
14		22.12	.488				
15		9.72	.420				
16		18.50	.406				
17		17.39	.384				
18		15.08	.331				
19		6.31	.272				
20		11.18	.360	622	3.789		
19 7dr 21	1208	7.69	.186	621	3.789	220.0 ± 5	

CLASSIFICATION

JPL 0000-5 (REV 11-68)

jpl →

PAGE 7 OF 9

(PREPARED BY) O. MAYNARD	(DATE) 3-4-75	(REPORT NO.)
(CHECKED BY) R. DICKINSON	(DATE)	(PROJECT)

TITLE SYSTEM TRANSFER EFFICIENCY DATA

SET NO.	TIME	V _{SET} , V	I _{SET} , A	PIVOTATED PA-FLOW	MAGNETRON E _h , Kv	I _h , mA	NOTES
19 7df 0	15:27	37.73	.287			240.0%	FREQ. ANO f _o = 2997.9
1		36.89	1.507				VSWR ANTENNA, dB 0.5
2		35.04	1.457				VSWR ARRAY RECTANG, dB
3		33.33	1.385				HORN-ANTENNA SAVING 170.2 CM.
4		59.18	1.275				RIPPLE V _h -I _h /V _{oc}
5		29.05	1.211				
6		25.93	1.094				
7		33.07	.711				
8		22.27	.936				
9		38.13	.827				
10		35.74	.773				
11		14.23	.606				
12		13.09	.574				
13		25.47	.562				
14		22.43	.500				
15		10.12	.444				
16		19.28	.431				
17		17.95	.397				
18		15.53	.339				
19		6.39	.279				
20		11.43	.372	656	3.766		
19 7df 01	15:33	7.94	.188	656	3.763		

CLASSIFICATION

JPL 0000-4 (REV 11-68)

(PREPARED BY) A. PARADIS/R. DICKINSON	(DATE) 3-4-75	(REPORT NO.)
(CHECKED BY)	(DATE)	(PROJECT) RXCV DC-RF-DC CERTIFICATION

TITLE SYSTEM TRANSFER EFFICIENCY DATA

SET NO.	TIME	RECTIFIER		PINNACULAR KX-FLURE	MAGNETRON		NOTES
		V _{SET} , V	I _{SET} , A		E _h , Kv	I _h , MA	
JPL 87 0	1650	37.31	1.284	669		240	FREQ. MHz f ₀ = 2446.9
1		36.78	1.514				VSWR Antenna, dB
2		34.96	1.460				VSWR ARRAY RECTIFIER, dB
3		33.40	1.393				Hard-Rectifier output 170.2 Hz CM.
4		58.87	1.267				RIPPLE V _{RM-TH} /SEC
5		27.88	1.174				Diode in set #7
6		24.75	1.058				replaced father
7		46.57	1.009				run.
8		21.16	.889				
9		37.02	.804				
10		34.51	.741				
11		14.85	.631				
12		13.44	.587				
13		³³ 26.27 ^{ap}	.575				
14		22.85	.507				
15		10.10	.440				
16		19.49	.426				
17		^{ap} 18.18	.401				
18		15.47	.337				
19		6.38	.279			3.780	
20		11.87	.383	657		3.805	
JPL 91 21	1655	8.03	.197	656		3.788	

jpl →

PAGE 9 OF 9

(PREPARED BY) R. Dickinson	(DATE) 3-4-75	(REPORT NO.)
(CHECKED BY) A. PARADIS	(DATE) 3-4-75	(PROJECT) RCLV DC-RF-DC CERTIFICATION
TITLE SYSTEM TRANSFER EFFICIENCY DATA		

SET NO.	TIME	Rectifier V _{SET} , V	I _{SET} , A	Power P _{AVG} , W	Wavelength λ, cm	I _{DC} , A	NOTES
① 0	17:49	36.10	.275	656	3.783	240.0 ± 2.0	FREQ. MHz f ₀ = 2446.8
1		35.73	1.963				VSWR Antenna, dB 0.5
2		33.80	1.414				VSWR ARRAY RECTIFIER, dB 1.0
3		32.28	1.326				MAX. RECTIFIER SPACING 181 cm.
4		57.20	1.236				RIPPLE V _{AVG} /V _{DC} 0.6/36
5		27.55	1.146				
6		29.44	1.026				I _C = 12 AMP.
7		46.05	.995				
8		21.14	.891				
9		37.42	.808				
10		34.74	.752				
11		19.85	.634				
12		14.14	.615				
13		27.44	.600				
14		24.00	.528				
15		10.65	.458				
16		20.35	.445				
17		19.47	.426				
18		17.04	.372				
19		7.07	.303				
20		13.74	.440	650	3.771		
② 21	17:55	8.94	.215	654	3.776	240 ± 4	

CLASSIFICATION

JPL 0000-5 (REV 11-68)

(PREPARED BY) R. DICKINSON	(DATE) 3-5-75	(REPORT NO.)
(CHECKED BY) A. PARADIS	(DATE) 3-5-75	(PROJECT) RXCV DL-AP-DC CERTIFICATION
TITLE MAGNETRON PERFORMANCE DATA & RF POWER MONITOR TRACKING		

TIME	I _b mA	E _b KV	FREQ. MHz	VSWR dB	INDICATED POWER		I _c A	E _c V
					DIGI-CAL W	HP-FWKE W		
JPL 87 1419	242.0	3.776	2448.0	0.208	631	659	11.6	3.5
1421	240.0	3.782	2448.0	0.2	620	650	11.6	3.5
1424	230.0	3.780	2445.8	0.3	598	626	11.6	3.6
1425	220.0	3.776	2445.0	0.2	568	597	11.7	3.6
1426	210.0	3.775	2443.2	0.2	540	564	11.7	3.6
1427	210.0	3.775	2443.5	0.2	542	567	11.7	3.6
1429	200.0	3.775	2442.7	0.2	515	541	11.7	3.7
1433	190.0	3.760	2441.2	0.3	486	512	11.7	3.7
JPL 87 1436	180.0	3.777	2440.5	0.2	458	483	11.8	3.7

MARK
18 MV PWR
535 MV/K

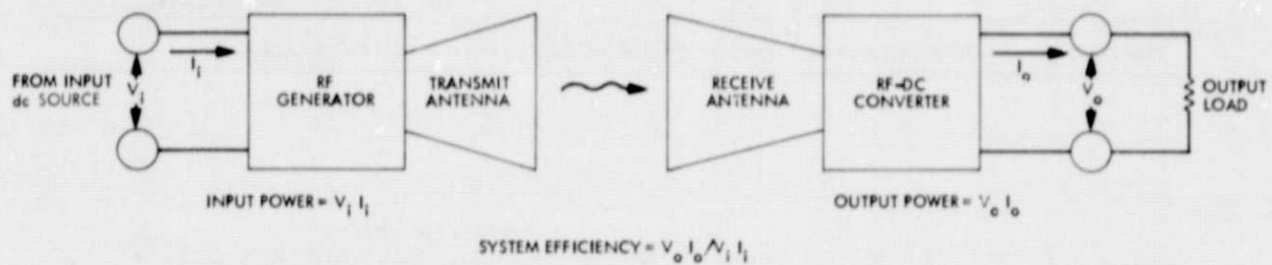


Fig. 1. Block diagram of microwave power transmission system

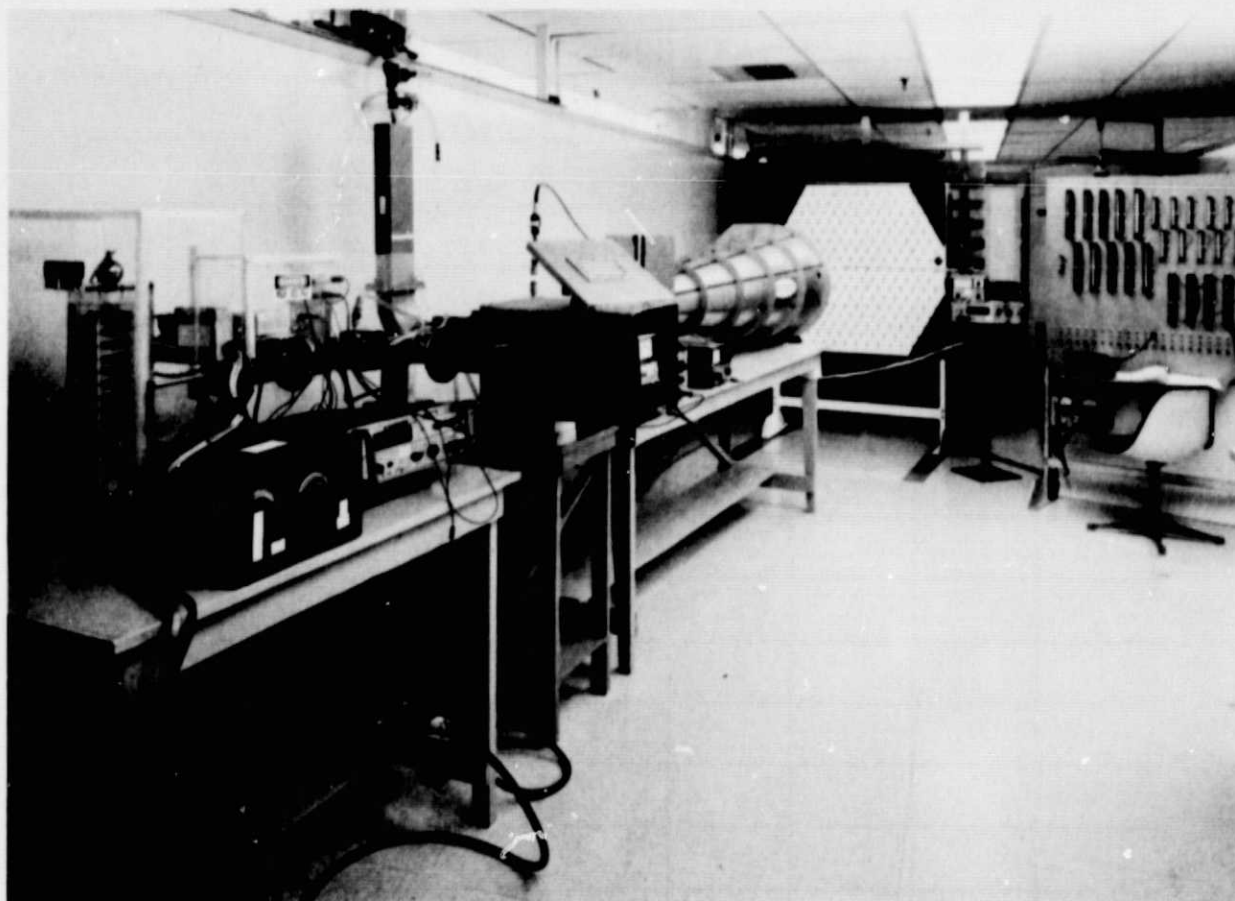
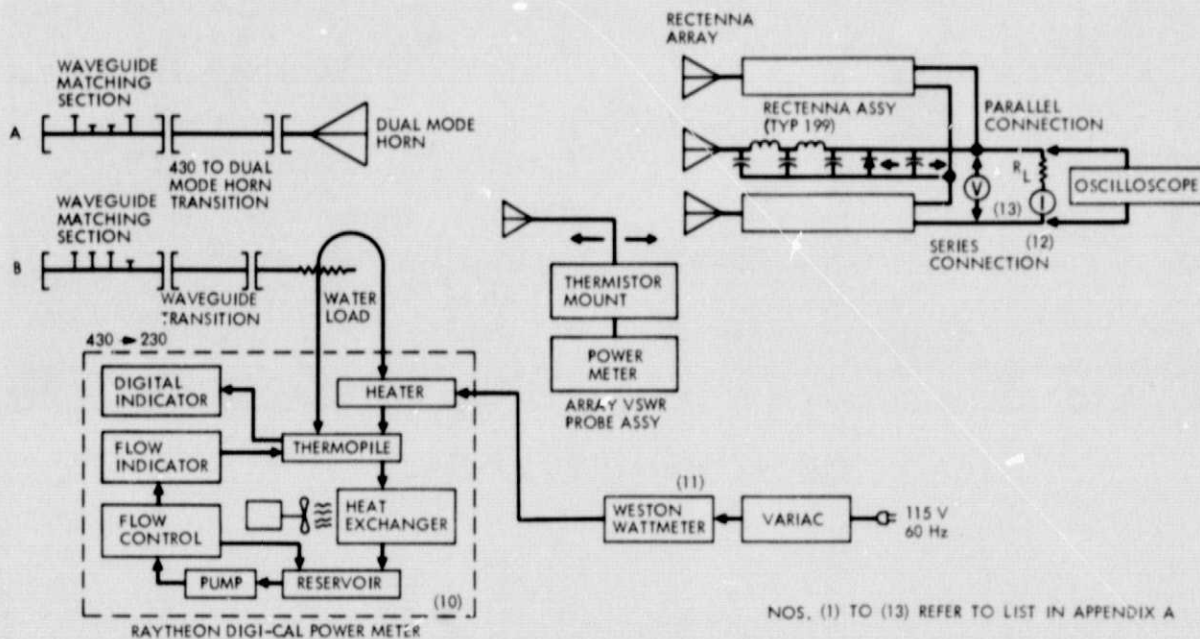
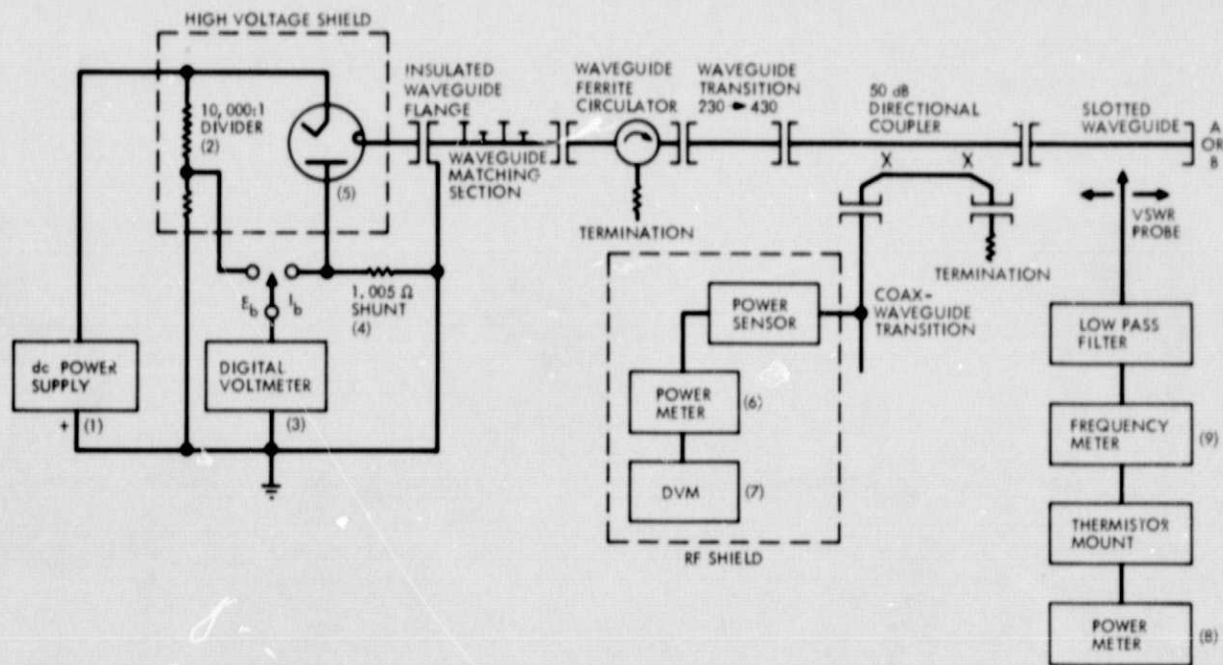


Fig. 2. Overall laboratory configuration



NOS. (1) TO (13) REFER TO LIST IN APPENDIX A

Fig. 3. Detailed system block diagram

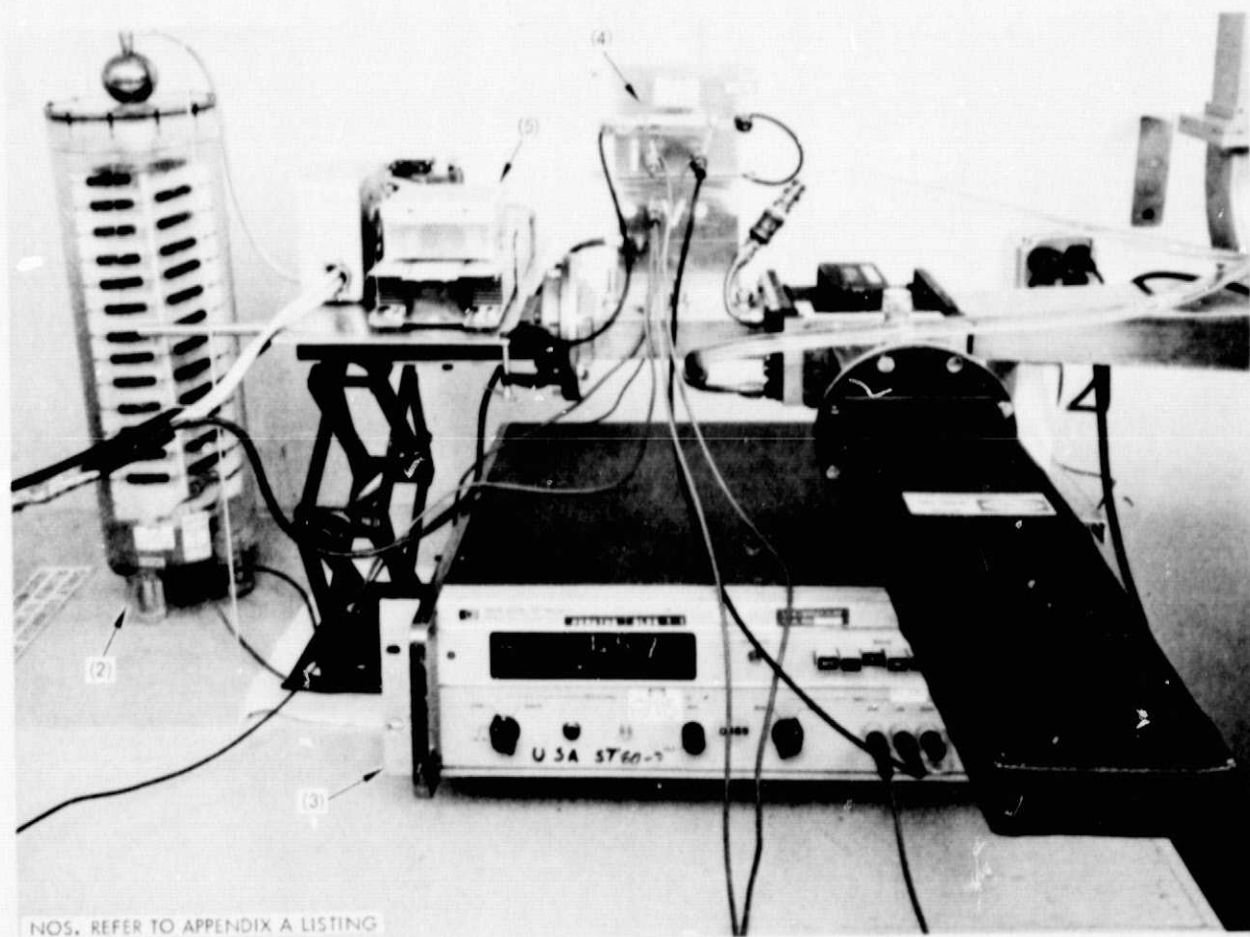


Fig. 4. Magnetron complex

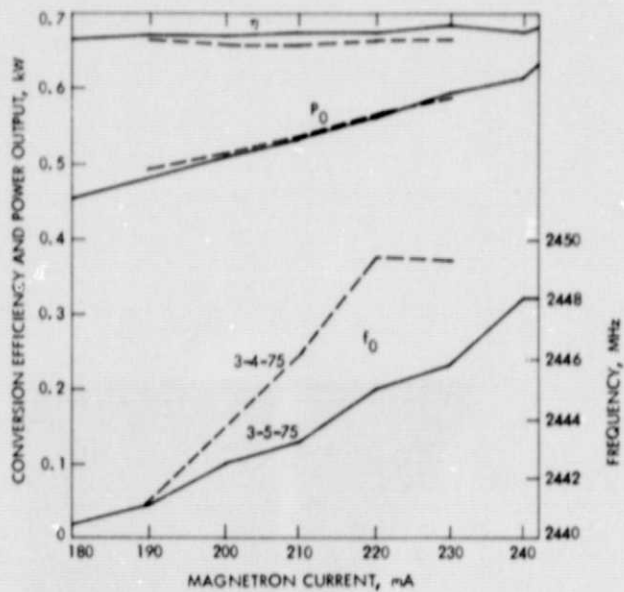


Fig. 5. Magnetron performance characteristics

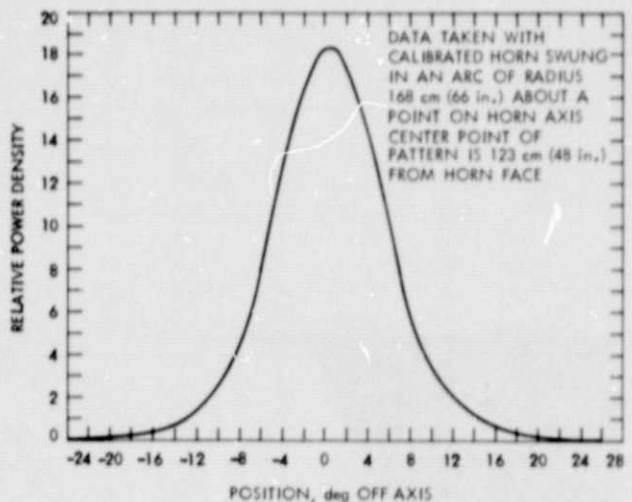


Fig. 6. Dual-mode horn antenna pattern

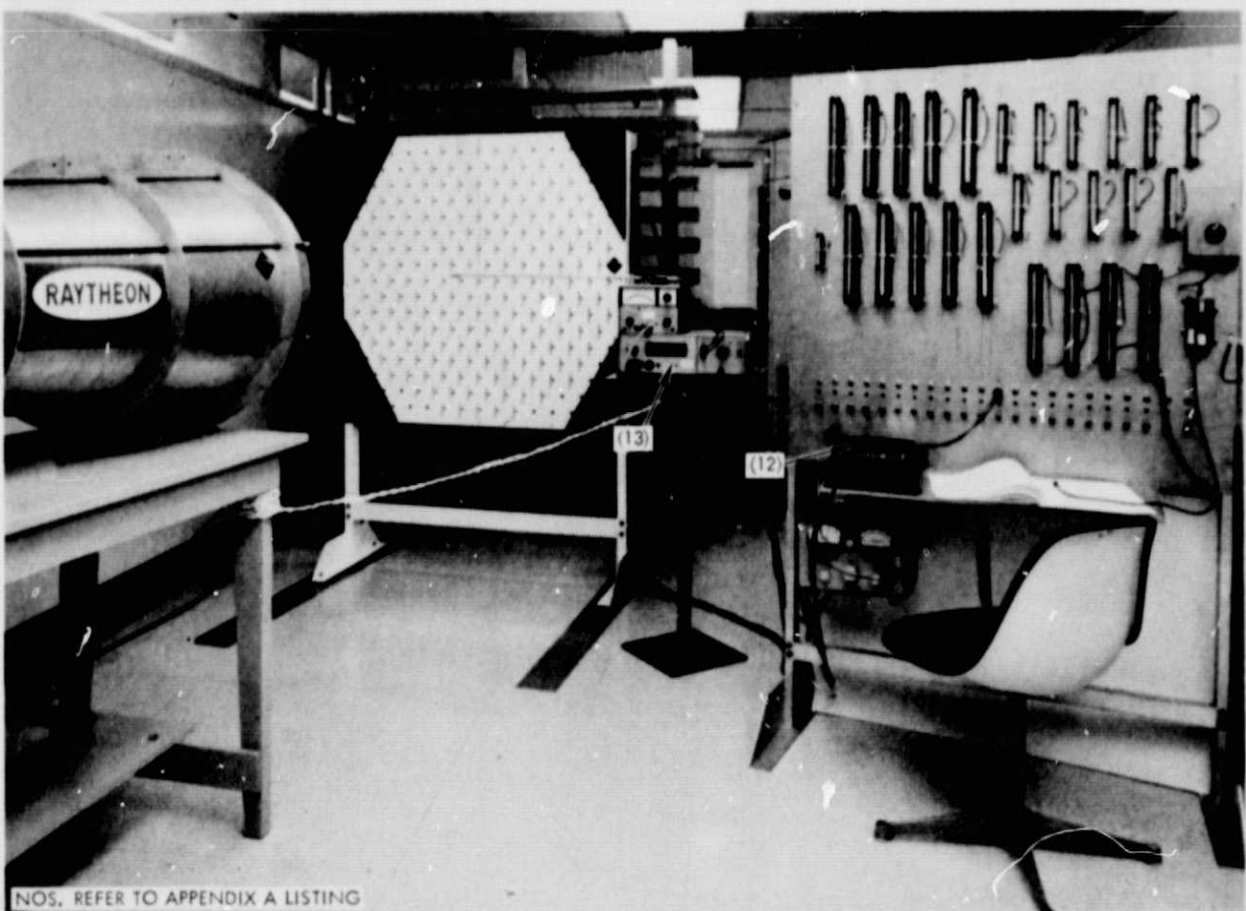


Fig. 7. Rectenna complex

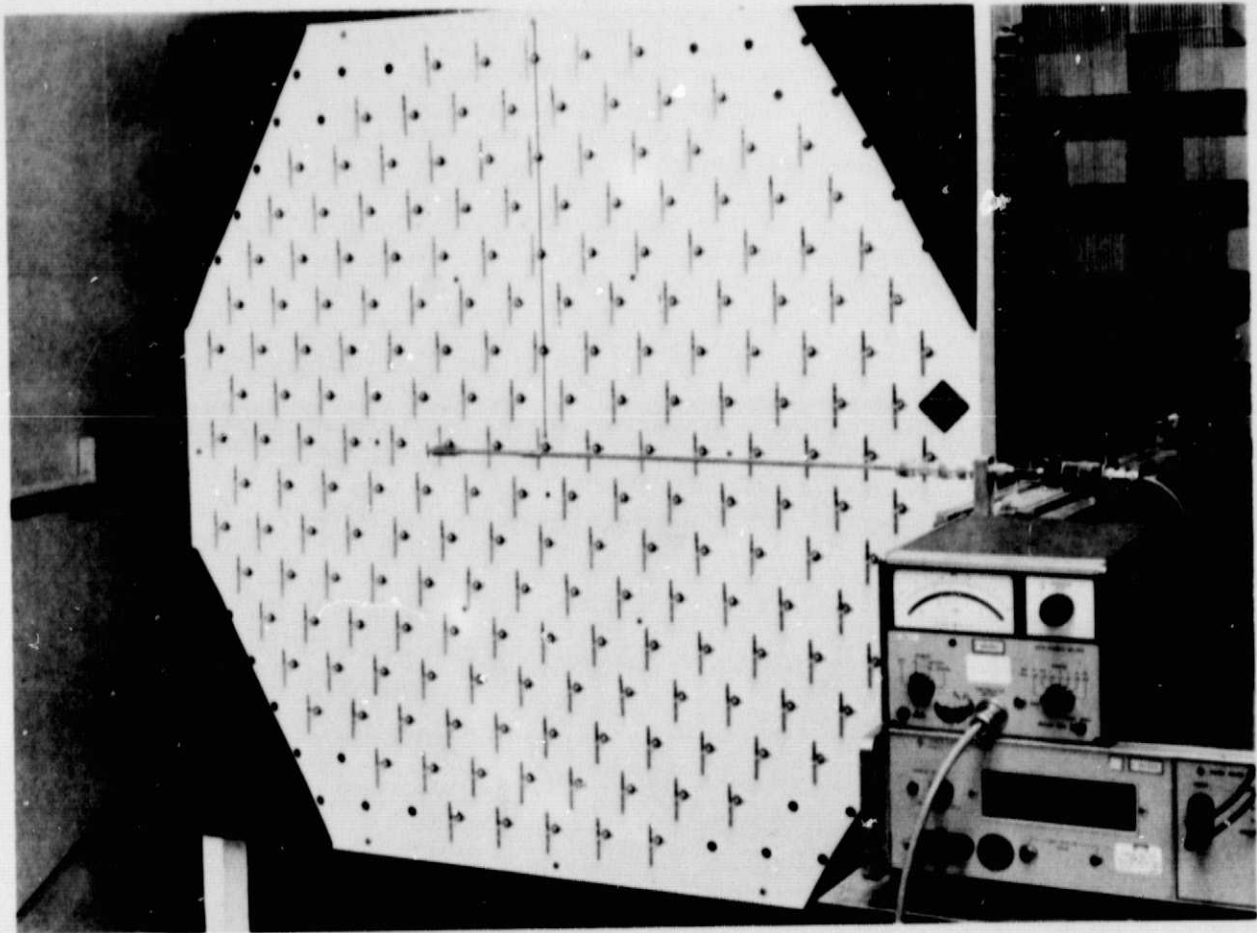
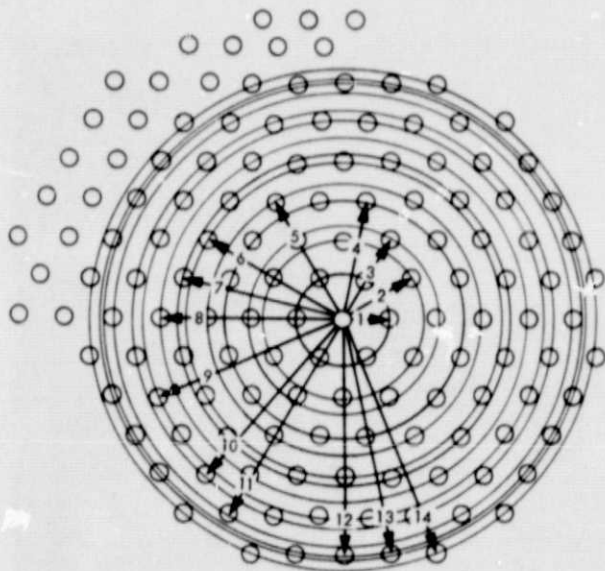


Fig. 8. Closeup view of receiving antenna



SET NO.	NO. IN SET
0	1 (CENTER)
1	6
2	6
3	6
4	12
5	6
6	6
7	12
8	6
9	12
10	12
11	6
12	6
13	12
14	12
15	6
16	12
17	12
18	12
19	6
20	18
21	12

Fig. 9. Rectenna element radial grouping

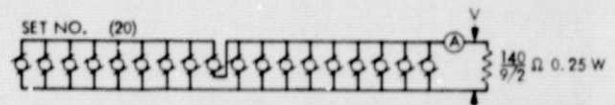
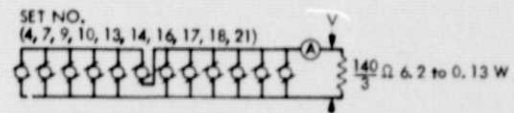
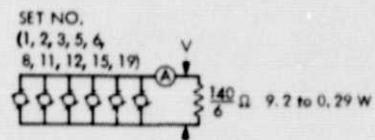
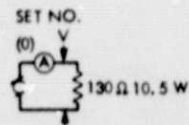


Fig. 10. Rectenna wiring format

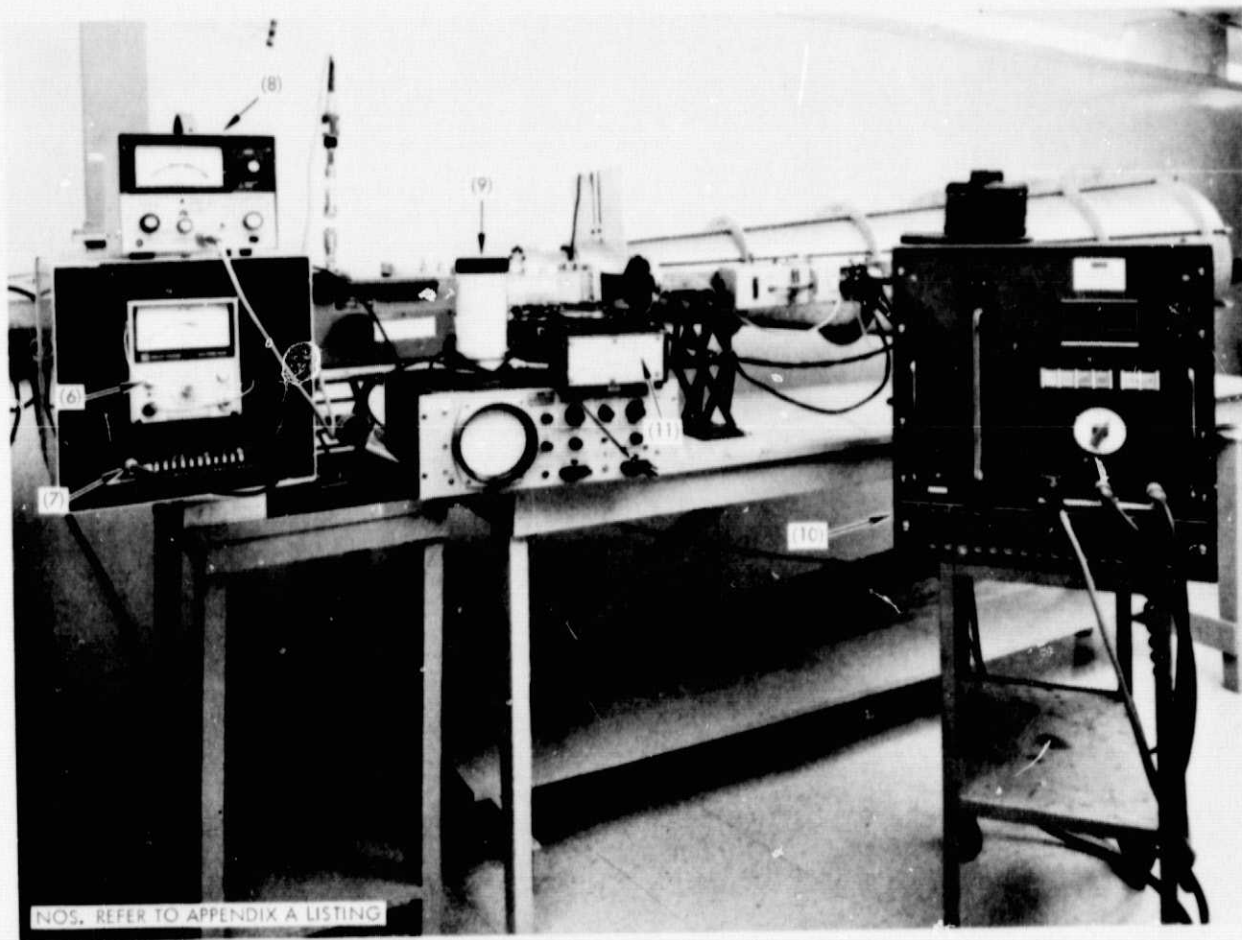


Fig. 11. Digi-Cal power meter complex

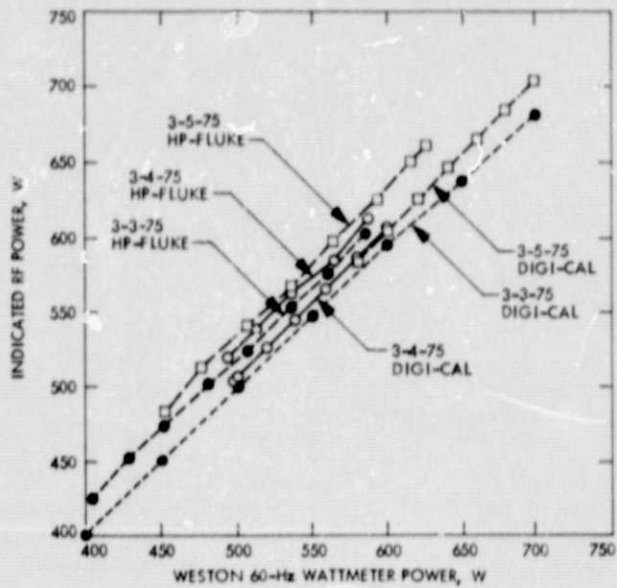


Fig. 12. Power meter calibrations

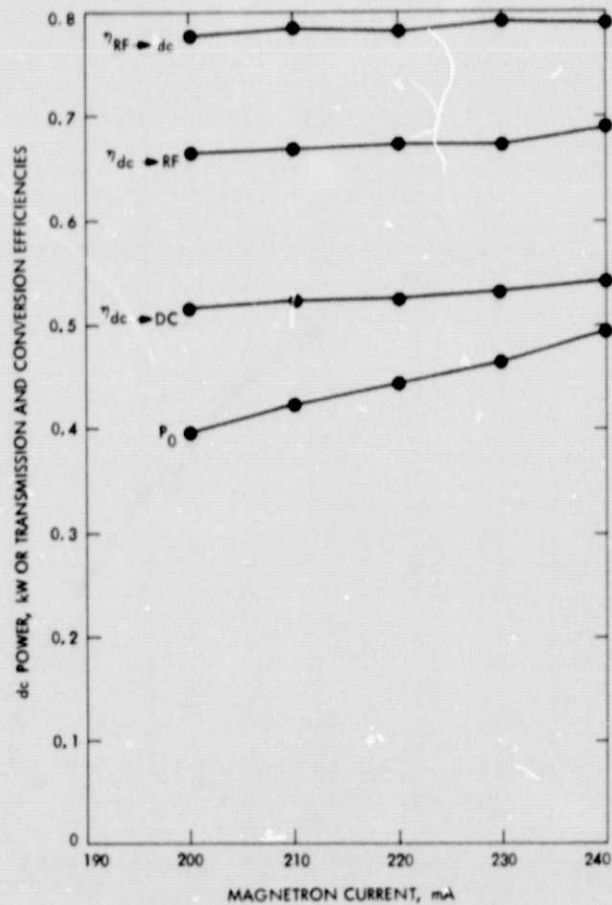
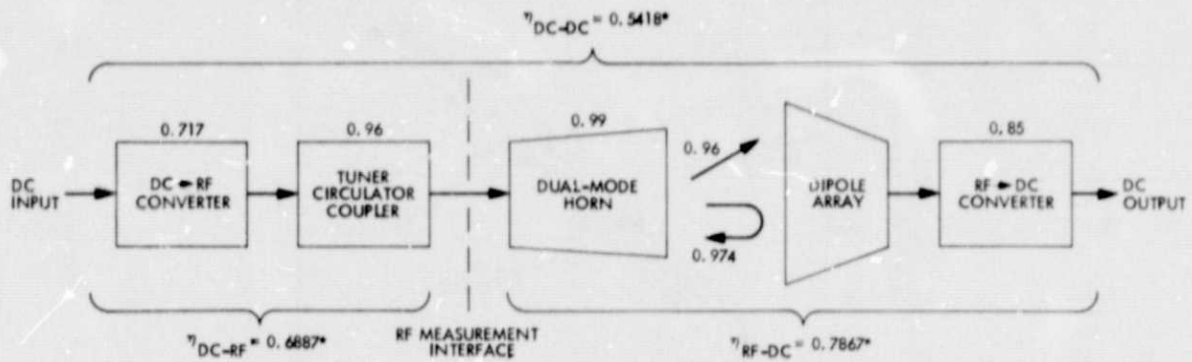


Fig. 13. System efficiency performance



LOSS CONTRIBUTORS

MAGNETRON CONVERSION, CIRCUIT AND REFLECTION LOSSES, HARMONICS, TUNER, CIRCULATOR, COUPLER AND SLOTTED GUIDE I^2R AND REFLECTION LOSSES.

LOSS CONTRIBUTORS

HORN AND ARRAY I^2R , POLARIZATION AND REFLECTION LOSSES. ARRAY SPILLOVER LOSS, DIODE CONVERSION LOSS

ESTIMATED PERCENT LOSSES

MAGNETRON	-28.3
DIODES	-15.0
SPILLOVER	-4.0
CIRCULATOR	-2.6
ARRAY MATCH	-2.6
HORN	-1.0

* MEASURED

Fig. 14. Distribution of system efficiencies (measured and estimated)

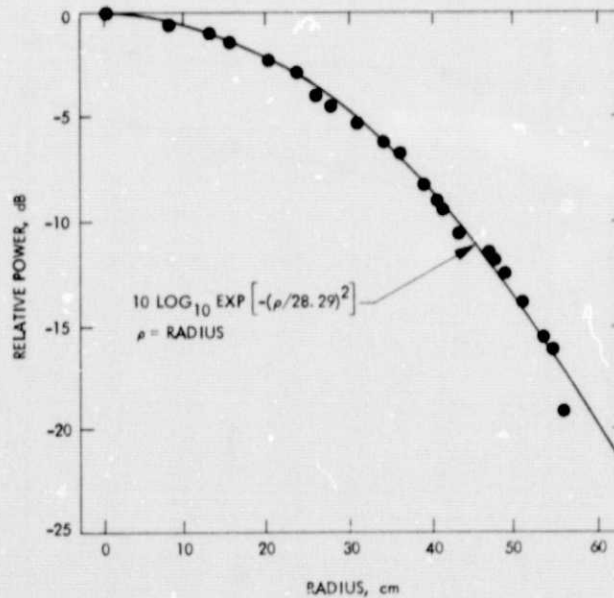


Fig. 15. Average power per element vs radius in the array